▌Radicals

Extremely Long Lived Localized Singlet Diradicals in a Macrocyclic Structure: A Case Study on the Stretch Effect

Yuta Harada,[a] Zhe Wang,[a] Shunsuke Kumashiro,[a] Sayaka Hatano,[a] and Manabu Abe*[a, b]

Abstract: Localized singlet diradicals have attracted much attention, not only in the field of bond-homolysis chemistry, but also in nonlinear optical materials. In this study, an extremely long lived localized singlet diradical was obtained by using a new molecular design strategy in which it is kinetically stabilized by means of a macrocycle that increases the molecular strain of the corresponding σ-bonded compound. Notably, the lifetime of this diradical (14 μs) is two orders of magnitude longer than that of a standard singlet diradical without a macrocyclic structure (≈ 0.2 μs) at 293 K. The species is persistent below a temperature of 100 K. In addition to the kinetic stabilization of the singlet diradical, the spontaneous oxidation of its corresponding ring-closed compound at 298 K produced oxygenated products under atmospheric conditions. Apparently, the "stretch effect" induced by the macrocyclic structure plays a crucial role in extending the lifetime of localized singlet diradicals and increasing the reactivity of their corresponding σ-bonded compounds.
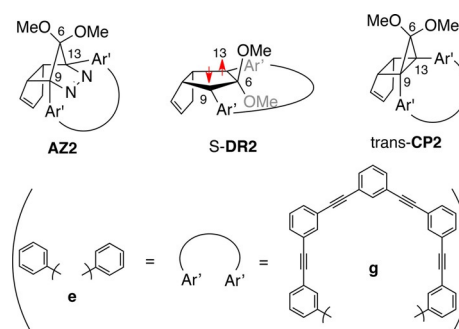
Introduction

Open-shell molecules with unpaired electrons have attracted considerable attention, not only in the field of reactive-intermediate chemistry[1] but also in nonlinear optical materials,[2] organic magnets,[3] luminescent materials,[4] and biological studies.[5] The three-dimensional and electronic structures of such high-energy molecules play a crucial role in their functionality. In general, however, the structure and reactivity of such species are experimentally elusive because of their short-lived character. Studies aimed at extending the lifetime of such reactive species are worthwhile to fully characterize their structure and reactivity, which give rise to their unique properties. Several studies on the isolation of highly energetic species such as carbenes,[6] radicals,[7] and delocalized diradicals[8] by means of kinetic and thermodynamic stabilization have been reported.

Localized diradicals are key intermediates in bond-homolysis processes.[9] The isolation of singlet diradicals has been reported in four-membered heterocyclic systems.[10] The ground-state spin multiplicity of propane-1,3-diyl diradicals **DR1** and the direct observation of singlet diradicals S-**DR2 a**–**f** have been in-

tensively investigated for over a decade.[11] The lifetime in benzene at 293 K has been reported to range from $\tau_{293} = 2$ ns to about 5500 ns depending on the substituents around the radical sites, which kinetically and/or thermodynamically stabilize the localized singlet diradicals. A unique nonlinear optical property has been also discovered for species with diradicaloid character.[12]

A new kinetic stabilization effect, termed the "stretch effect",[13] on the reactivity of the localized singlet diradical S-**DR2 g,h** was designed and examined in the present study. Notably, laser flash photolysis (LFP) experiments on the precursor azo alkanes **AZ2 g,h** (Scheme 1) revealed that the lifetimes of S-**DR2 g,h** are roughly two orders of magnitude longer ($\tau_{293} \approx 14$ μs) than that of S-**DR2 e**[14] ($\tau_{293} \approx 0.2$ μs). The intermolecular reactivity of the extremely long lived singlet diradical S-**DR2 h** was also investigated in this study.

[a] Y. Harada, Z. Wang, S. Kumashiro, S. Hatano, Prof. M. Abe
Department of Chemistry, Graduate School of Science
Hiroshima University, 1-3-1 Kagamiyama
Higashi-Hiroshima, Hiroshima 739-8526 (Japan)
E-mail: mabe@hiroshima-u.ac.jp

[b] Prof. M. Abe
Hiroshima University Research Center for
Photo-Drug-Delivery Systems (HiU-P-DDS), 1-3-1 Kagamiyama
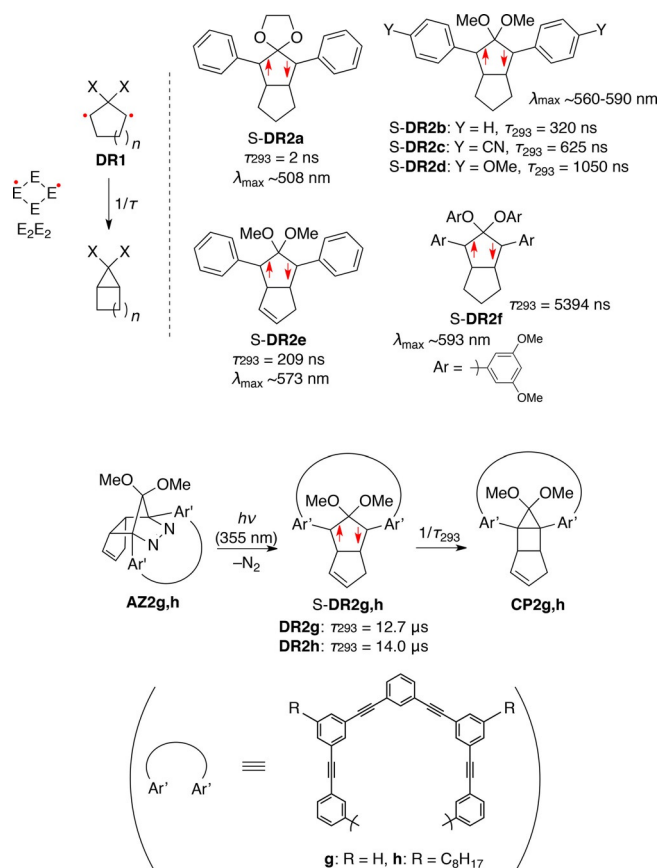Higashi-Hiroshima, Hiroshima 739–8526 (Japan)

Results and Discussion

Synthesis of azo alkane AZ2 g,h

Azoalkanes **AZ2 g,h**, the precursors of **DR2 g,h**, were synthesized with Hünig[15] and inter- and intramolecular Sonogashira

Scheme 1. Macrocyclic effect on the reactivity of localized singlet diradicals.

cross-coupling[16] reactions as the key steps (Scheme S1 in the Supporting Information). The n,π* electronic transition of the azo chromophore was observed at 359 ($\varepsilon = 183$) and 358 nm ($\varepsilon = 171$ dm^3 mol^{-1} cm^{-1}) in benzene for **AZ2 g** and **AZ2 h**, respectively (Figure S1 in the Supporting Information). The molar extinction coefficients ε at about 360 nm were somewhat larger than that of a typical azo chromophore. For example, the ε value of **AZ2 b**, which is the precursor of **DR2 b**, in benzene has been reported to be about 112 at 367 nm, and this indicates that the ε values of **AZ2 g,h** contain a contribution from the 1,3-diacetylphenyl chromophore. A high-quality single crystal of **AZ2 g** was obtained by recrystallization, and the macrocyclic structure of **AZ2 g** was confirmed by single-crystal X-ray crystallographic analysis (Figure 1). Table 1 lists
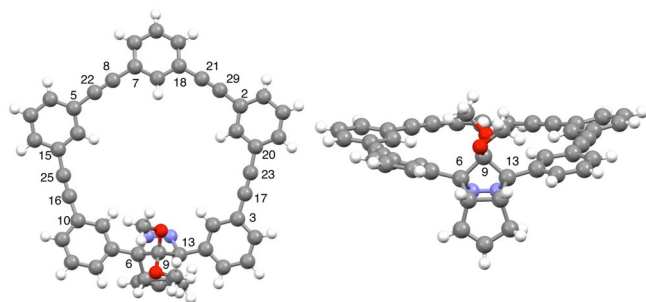

Figure 1. Top and side views of the X-ray crystallographic structure of **AZ2 g**.

Table 1. Experimental and computed structural data[a] for **AZ2 e,g**,[b] **DR2 e,g**,[c] and *trans*-**CP2 e,g**.[b]

Entry		AZ2 e_exptl / AZ2 g_exptl	AZ2 e_calcd / AZ2 g_calcd	S-DR2 e_calcd / S-DR2 g_calcd	*trans*-CP2 e_calcd / *trans*-CP2 g_calcd
1	C9—C13	2.255 / 2.264	2.269 / 2.269	2.389 / 2.389	1.547 / 1.583
2	C9-C6-C13	91.73 / 92.51	91.92 / 91.75	103.93 / 103.78	61.57 / 63.15
3	C10-C16-C25	– / 175.68	– / 175.20	– / 179.12	– / 176.06
4	C16-C25-C15	– / 175.36	– / 174.47	– / 178.32	– / 169.37
5	C5-C22-C8	– / 176.44	– / 175.82	– / 176.25	– / 169.76
6	C22-C8-C7	– / 175.38	– / 176.58	– / 174.84	– / 169.56
7	C18-C21-C29	– / 176.63	– / 177.02	– / 174.87	– / 173.38
8	C21-C29-C2	– / 174.61	– / 177.10	– / 176.34	– / 177.75
9	C20-C23-C17	– / 175.81	– / 176.48	– / 178.30	– / 178.35
10	C23-C17-C3	– / 177.18	– / 176.30	– / 179.17	– / 176.27

[a] Bond lengths in Ångstroms, angles in degrees. [b,c] Optimized at (R)B3LYP/6-31G(d) and (U)B3LYP/6-31G(d) levels of theory, respectively.

the C9—C13 distance in **AZ2 g**, which becomes the radical center after denitrogenation, and selected bond angles. Slightly bent structures were observed for the four triple bonds: C10-C16-C25 175.68° (Table 1, entry 3), C16-C25-C15 175.36° (Table 1, entry 4), C18-C21-C29 176.63° (Table 1, entry 7), and C21-C29-C2 174.61° (Table 1, entry 8). The experimentally obtained values were well reproduced by optimizing the geometry of **AZ2 g** at the B3LYP/6-31G(d)[17] level of theory (Table 1). For instance, the experimental and calculated C9—C13 distances were very similar (2.264 and 2.269 Å, respectively; Table 1, entry 1). The slightly bent triple bond ($\approx 175°$) was also well reproduced by the calculations.

Macrocyclic effect on the molecular structures

The singlet diradical S-**DR2 g** and its ring-closed compound *trans*-**CP2 g** were also computed at the (R,U)B3LYP/6-31G(d) level of theory (Table 1). The distance between the radical centers at C9 and C13 in S-**DR2 g** was calculated to be 2.389 Å, which is longer than that in **AZ2 g** (Table 1, entry 1). The C9-C6-C13 angle in the propane-1,3-diyl moiety was larger than

that of **AZ2g** (Table 1, entry 2), which is consistent with the longer distance between C9 and C13 (Table 1, entry 1). The triple bonds in S-**DR2g** were found to be more linear than those in **AZ2g** (Table 1, entries 3–10). For example, the C10-C16-C25 and C16-C25-C15 angles in S-**DR2g** were 179.12 and 178.32°, respectively, whereas they were 175.20° and 174.47° in **AZ2g** (Table 1, entries 3,4). In contrast to the linear triple bond in S-**DR2g**, relatively distorted triple bonds were computed in the ring-closed compound *trans*-**CP2g** (Table 1, entries 3–10). For example, the angles C5-C22-C8, C22-C8-C7, and C18-C21-C29 were found to be 169.76, 167.56, and 173.38° in **CP2g** (Table 1, entries 5–7).

To examine the macrocyclic effect more fully, the structures of **AZ2e**, S-**DR2e**, and *trans*-**CP2e**, which have no macrocyclic ring, were compared with those of **AZ2g**, S-**DR2g**, and *trans*-**CP2g** (Table 1, entries 1 and 2). As expected, the distance between the two azo carbon atoms C9 and C13 in **AZ2g** (2.264 Å) was slightly longer than that of the related azo carbon atoms in **AZ2e** (2.255 Å). The single-crystal X-ray structure of **AZ2e** is shown in Figure S2 of the Supporting Information. In addition to the effect on the carbon–carbon distance, the C9-C6-C13 bond angle in **AZ2e** (91.73°) is smaller than that in **AZ2g** (92.51°), that is, the macrocyclic ring system pulls C9 and C13 in opposite directions in **AZ2g** (Figure 2). This
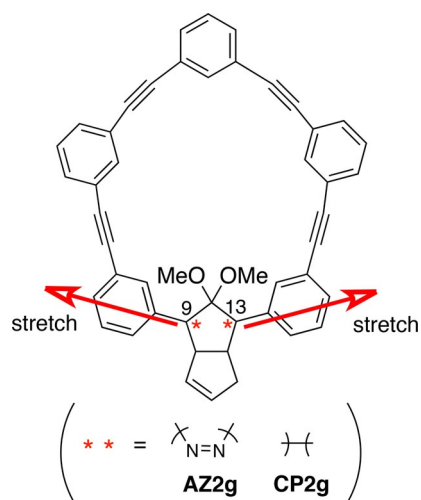

Figure 2. Stretch effect induced by a macrocyclic system.

macrocyclic effect was also observed more significantly in the computed ring-closed structure *trans*-**CP2**, although the distance in S-**DR2** was calculated to be nearly identical for S-**DR2e** and S-**DR2g** (Table 1, entries 1 and 2). The distance in **CP2g** (1.583 Å) was found to be longer than that in **CP2e** (1.547 Å), that is, the two carbon atoms in **CP2g** are pulled in opposite directions because of the macrocyclic ring strain (Figure 2). This new kinetic stabilization effect induced by the macrocyclic ring is expected to extend the lifetime of the singlet diradical S-**DR2g** and the reactivity of the ring-closed compound **CP2g** relative to S-**DR2e** and **CP2e**.

The bending effect θ of the triple bonds on the destabilization energy was estimated by means of the angle-dependent

energy change of 1,2-diphenylethyne at the B3LYP/6-31G(d) level of theory (Figure 3). The total electronic energy at 175° was 2 kJ mol^{-1} higher than that at 180°. Energetic destabilizations of 8, 18, and 33 kJ mol^{-1} were computed for angles of 170, 165, and 160, respectively, for one diphenylethyne moiety.
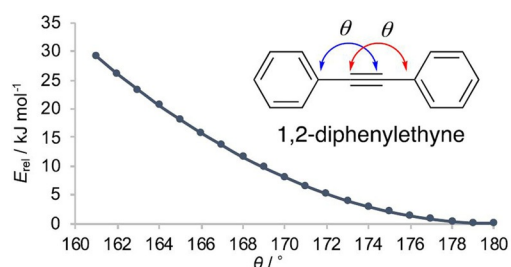

Figure 3. Bending effect on the energetic destabilization of the 1,2-diphenylethyne moiety.

To further investigate the macrocyclic effect on the energetic destabilization of **CP2g**, the energy difference between the singlet diradicals S-**DR2g** and **CP2g** was computed at the B3LYP/6-31G(d) level of theory and compared with that of S-**DR2e** and **CP2e** (Table 2). As expected for the stretch effect, induced by the strain of bending the triple bond in the system (Table 1, Figure 3), the enthalpy differences for S-**DR2g** and **CP2g** with macrocyclic structures [i.e., −20.9 (*trans* isomer) and −0.5 (*cis* isomer)] were found to be much smaller than those of S-**DR2e** and **CP2e** [i.e., −36.9 (*trans* isomer) and −13.7 (*cis* isomer)]. Consistent with the destabilization of ring-closed compound **CP2g**, the transition-state energies from singlet diradical S-**DR2g** to *trans*- and *cis*-**CP2g** (68.5 and 50.3 kJ mol^{-1}, respectively) were larger than those for the reac-

Table 2. Macrocyclic effect on ΔH_{rel} (ΔE_{rel})[a] in **CP2e** and **CP2g**.

	ΔH_{rel} (ΔE_{rel}) [kJ mol^{-1}]					
	S-**DR**	T-**DR**	*trans*-**CP**	*cis*-**CP**	TS$_{trans}$/ν_i[b]	TS$_{cis}$/ν_i[b]
2e	0.00	17.5	−36.87	−13.74	63.58 (66.18)/	44.18 (45.96)/
	(0.00)	(17.2)	(−36.53)	(−9.67)	−329.33	−371.65
2g	0.00	17.1	−20.85	−0.53	68.54 (71.23)/	50.31 (53.07)/
	(0.00)	(16.7)	(−19.89)	(0.38)	−45.09	−36.32

[a] Optimized at the (R,U)B3LYP/6-31G(d) level of theory. [b] The values of ν_i are imaginary frequencies computed at the same level of theory.

tion from **DR2e** without the macrocyclic ring to *trans*- and *cis*-**CP2e** (63.6 and 44.2 kJ mol^{-1}, respectively), that is, S-**DR2g** is kinetically stabilized by the macrocyclic ring. As previously found for S-**DR2b**, formation of *cis*-**CP2e** and *cis*-**CP2g** was predicted to be energetically more favorable than formation of the *trans* isomers.[9n] Thermal isomerization from the *cis* to the *trans* isomer appears to be possible for *cis*-**CP2g** at 298 K; indeed, the activation enthalpy for the transition from S-**DR2g** to *trans*-**CP2g** is computed to be 68.5 kJ mol^{-1}, as observed for the thermal isomerization from *cis*-**CP2b** to *trans*-**CP2b**.[9n] The singlet ground states of **DR2e** and **DR2g** were also confirmed by the computations as $\Delta E_{ST} = E_S - E_T \approx -17$ kJ mol^{-1} (Table 2).

UV/Vis and EPR studies on the photolysis of AZ2e,g,h and 16

Transient absorption spectroscopic analyses were conducted following LFP of **AZ2g** (5 mg, 2.5 mM, Abs$_{355}$ = 0.46) and **AZ2h** (6 mg, 2.4 mM, Abs$_{355}$ = 0.48) in benzene with an Nd:YAG laser (λ_{exc} = 355 nm, 5 ns pulse, 7 mJ) at 293 ± 0.1 K (Figure 4). Under

an N$_2$ atmosphere, two transient species were observed at about 480 and about 580 nm for **AZ2g** and decayed with first-order kinetics (Figure 4a). The lifetimes of the species were determined to be 2.1 ± 0.1 and 12.7 ± 1.1 µs by single-exponential kinetic fitting. Under air, only the transient species at about 580 nm was observed with a small band at about 460 nm (Figure 4b) and also decayed with first-order kinetics with lifetimes of 14.0 ± 1.1 and 13.8 ± 1.2 µs, respectively. The nearly equal lifetimes at 580 and 460 nm clearly indicate that the two bands are derived from the same species. The nearly identical lifetime under an N$_2$ atmosphere indicates that the species at 480 nm is a triplet and that at 580 nm is a singlet. The absorption maximum of localized singlet diradicals **DR2** typically occur at about 500–600 nm.[11] The absorption band corresponds to a π-to-π* electronic transition of the π–single bonding system (C-π-C).[18] All the experimental evidence suggests that the transient species at 580 nm is the singlet diradical S-**DR2g**. The lifetime of S-**DR2g** ($\approx$14 µs at 293 K) was almost two-orders of magnitude longer than that of parent compound S-**DR2e** (209 ns at 293 K).[14] As expected owing to the stretch effect induced by the macrocyclic system (Figure 2), S-**DR2g** is highly kinetically stabilized as an extremely long lived localized singlet diradical.

To gain additional insight into the triplet species observed at about 480 nm in the LFP experiment (Figure 4a), the UV/Vis absorption spectrum for the photolysis of **AZ2g** was recorded under low-temperature glassy-matrix conditions for a solution of **AZ2g** in degassed 2-methyltetrahydrofuran (MTHF). Two bands were observed, at about 470 and about 580 nm during the photolysis of **AZ2g** in the MTHF glassy matrix at 90 K (Figure 5a). After 3 min of photolysis, the $\approx$470 nm species decayed under dark conditions, whereas the 580 nm species having the low-intensity band at $\approx$460 nm persisted. These phenomena clearly indicate that the 470 nm species is an electronically excited state that has a T–T absorption at about 470 nm, and the 580 nm species with 460 nm is a reactive intermediate (i.e., S-**DR2g**) that is existent at low temperature.

To confirm the spin multiplicity of the 470 and 580 nm species, low-temperature EPR spectroscopic and phosphorescence analyses were conducted under similar conditions to those used for the UV/Vis absorption measurements (Figures 5b). During the photolysis of **AZ2g** with a 365 nm LED, triplet EPR signals were observed at 1512, 2049, 2682, 3944, and 4676 G. The high-intensity signal at 1512 G corresponds to the half-field transition ($m_s = \pm 2$) of the allowed transitions ($m_s = \pm 1$) at 2049 (*z*), 2682 (*x,y*), 3944 (*x,y*), and 4676 (*z*), from which the zero-field splitting parameters D/hc and E/hc were determined as 0.123 and < 0.001 cm^{-1}, respectively. An accurate E value was difficult to obtain owing to the broad x and y signals. The large D value suggests that the triplet state is not derived from the 1,3-diradical moiety but from a benzene moiety. The typical D value for triplet 1,3-diphenylpropane-1,3-diyl diradical species is known to be about 0.05 cm^{-1};[19] D values of about 0.12–0.15 cm^{-1} have been reported for the triplet state of benzene derivatives such as benzene itself[20] and 1,3-dicyanobenzene.[21] Disappearance of the typical triplet signals under dark conditions indicated that they were derived from the 470 nm
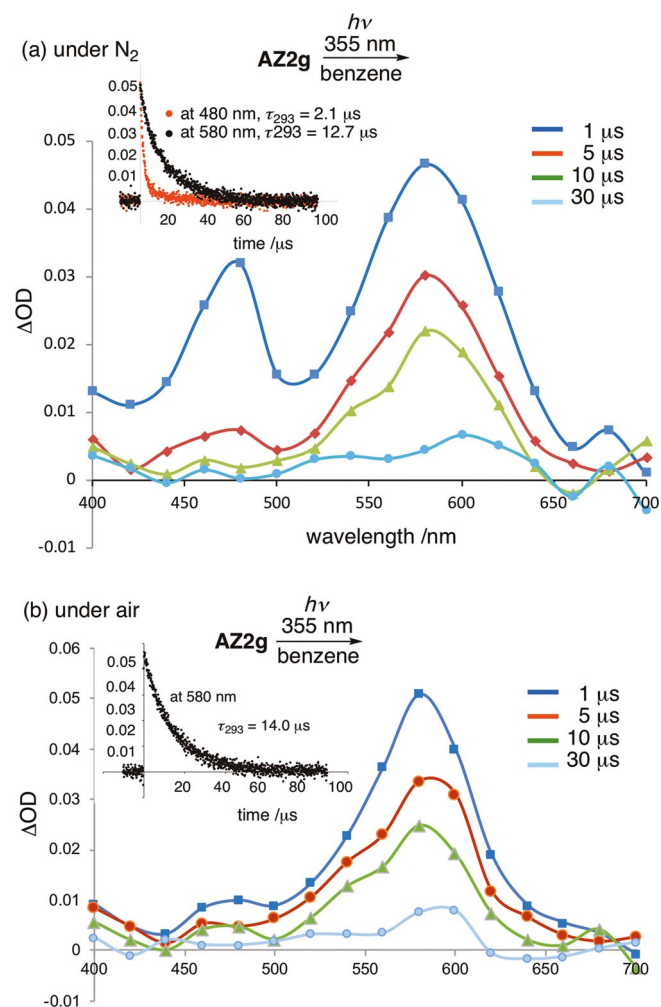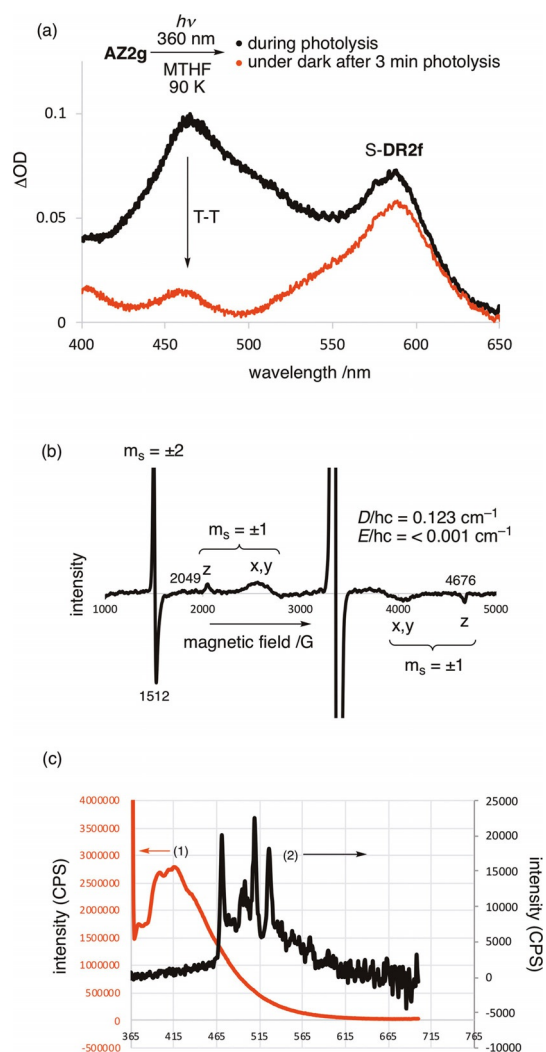

Figure 4. Transient absorption spectra for the LFP (293 K, benzene) of a) **AZ2g** (5 mg, 2.5 mM, Abs$_{355}$ = 0.46) under N$_2$ conditions. Inset: time profiles of the 480 and 580 nm species. b) **AZ2g** (5 mg, 2.5 mM, Abs$_{355}$ = 0.46) under atmospheric conditions. Inset: time profile of the 580 nm species.

Figure 5. a) UV/Vis spectroscopic analysis of the photolysis of **AZ2g** with an Xe lamp (360 ± 10 nm) in an MTHF matrix at 90 K. b) EPR spectroscopic analysis during the photolysis of **AZ2g** in an MTHF matrix at 80 K. c) 1) Fluorescence spectrum of **AZ2g** (0.12 mM, $\lambda_{exc} = 360$ nm) in MTHF at 77 K; 2) Phosphorescence spectrum of **AZ2g** (0.12 mM, $\lambda_{exc} = 360$ nm) in MTHF at 77 K.

the absorbance at about 360 nm occurs for the mixture of azo and 1,3-diacetylphenyl chromophores (cf. the ε values for **AZ2g,h**). After 5 min of irradiation at 365 nm with an LED, no triplet EPR signals were observed under dark conditions, although purple-colored 580 nm species were clearly observed by UV/Vis spectroscopy (Figure 5a). This observation provides evidence that the 580 nm species is the singlet state of the localized diradical S-**DR2g**.

A similar transient absorption spectrum was also observed in the LFP study on **AZ2h** (R = C_8H_{14}, Figure S3) under air. The lifetime of the 580 nm species, **DR2h**, was determined as 14.2 ± 0.8 μs at 293 K in benzene, which is nearly identical to that of **DR2g** and indicates a negligible alkyl-chain effect on the lifetime. The temperature-dependent change of the lifetime of S-**DR2g,h** (Figures S3 and S4 in the Supporting Information) gave activation parameters (E_a, lg A, $\Delta H^{\neq}$, $\Delta S^{\neq}$, $\Delta G^{\neq}_{293}$) for the ring-closing process of the singlet diradicals S-**DR2g,h** to **CP2g,h** from Eyring and Arrhenius plots at temperatures between 283 and 313 K (Table 3). The activation energy and enthalpy of the decay process of S-**DR2g,h** were found to be about 20 kJ mol^{-1} higher than those of **DR2e**, that is, the singlet diradicals are kinetically stabilized by the macrocyclic ring. To understand the substituent effect at the *meta* positions in S-**DR2g,h** on the lifetime, an LFP study on compound **16** with two arylacetyl substituents at the *meta* positions, which is the byproduct in the synthesis of **AZ2h**, was also performed (Scheme S1 in the Supporting Information, Scheme 2, Table 3). The lifetime of the singlet diradical S-**DR16** was found to be 620 ± 12 ns at 293 K (Figure S5 in the Supporting Information), which is much shorter than that of S-**DR2g,h** with the macrocyclic system (Table 3). As judged by the large lg A values of about 12, the decay of 580 nm species is spin-allowed process to give the corresponding singlet products (Scheme 2).[22] The activation energies of the first-order decay process of **DR2g,h** were found to be about 52–55 kJ mol^{-1}, which are close to the computed values for the ring-closing reaction to the *cis* isomer of the ring-closure product *cis*-**CP2g** (Table 2). The negligible substituent effect of the *meta* substituents on the thermodynamic stabilization of the diradical was revealed by the similar absorption maxima of S-**DR2e**, S-**DR2g**, and S-**DR16**, which were found to be 575, 575, and 576 nm. Furthermore, the computed spin density of 0.735 at the benzylic position of the triplet state of **DR2e** was also similar to that of 0.736 for T-**DR2g** at the UB3LYP/6-31G(d) level of theory, and thus indicated a negligible *meta*-substituent effect on the thermodynamic stability of **DR2**.

species. In fact, structured phosphorescence was observed at $\lambda_{0-0} \approx 470$ nm following 360 nm excitation of **AZ2h** (0.12 mM) in MTHF at 77 K together with fluorescence at $\lambda_{0-0} \approx 370$ nm (Figure 5c). The concomitant generation of the triplet state of the di-*meta*-substituted benzene moiety at about 470 nm with the singlet diradical **DR2g** at 580 nm is reasonable, because

Table 3. Lifetime τ_{293} and activation parameters (E_a, lg A, $\Delta H^{\neq}$, $\Delta S^{\neq}$, $\Delta G^{\neq}_{293}$) of S-**DR2e,g,h** and S-**DR16**.

DR	τ_{293} [μs][a]	E_a[b] [kJ mol^{-1}]	lg A [s^{-1}][b]	$\Delta H^{\neq[c]}$ [kJ mol^{-1}]	$\Delta S^{\neq[c]}$ [J K^{-1} mol^{-1}]	$\Delta G_{293}^{\neq[c]}$ [kJ mol^{-1}]
DR2e	0.209 ± 0.012	30.5 ± 0.4	12.1 ± 0.1	28.0 ± 0.4	−21.5 ± 0.8	34.2 ± 0.8
DR2g	14.0 ± 1.1	55.4 ± 0.7	14.7 ± 0.2	52.9 ± 0.7	28.4 ± 3.2	44.6 ± 0.9
DR2h	14.2 ± 0.8	52.3 ± 0.4	14.1 ± 0.1	49.7 ± 0.4	17.1 ± 1.2	44.7 ± 0.4
DR16	0.620 ± 0.012	31.2 ± 0.8	11.7 ± 0.1	28.7 ± 0.8	−28.9 ± 2.7	37.2 ± 0.8

[a] In benzene at 293 K; errors are standard derivations from five data points. [b, c] Determined by Arrhenius plots and Eyring plots, respectively, of the lifetimes of singlet diradicals monitored at 580 nm at five temperatures between 283 and 313 K.
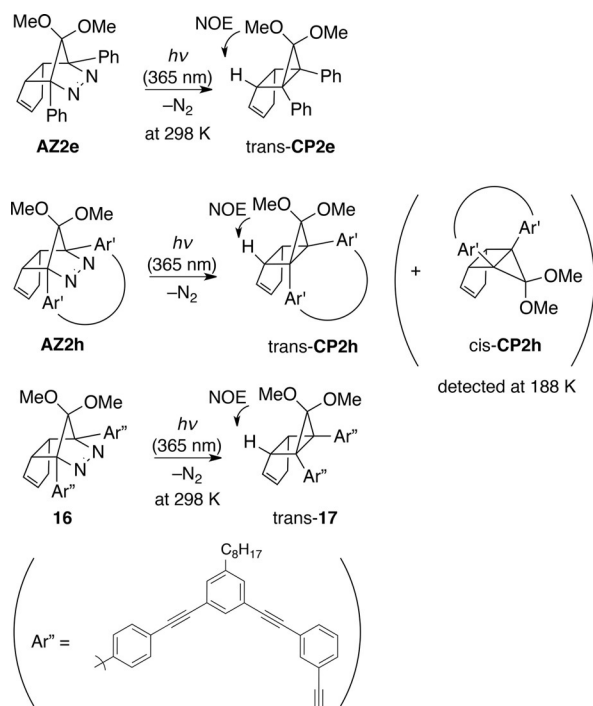
Scheme 2. Product analysis of azoalkanes **AZ2 e**, **AZ2 h**, and **16** in photochemical denitrogenation in benzene at 298 K.

Product analysis in the photolysis of AZ2 e,h and 16 and intermolecular reactivity of CPe,h, and 17

Product analysis of the photochemical reactions of **AZ2 e**, **AZ2 h**, and **16** was conducted at 365 nm by using a LED in a sealed degassed NMR tube containing a C_6D_6 solution of azo alkane at 298 K. The photolysate was directly analyzed by ^{1}H and ^{13}C NMR spectroscopy (Scheme 2, Figure 6, and Figures S6 and S7 in the Supporting Information). The NMR analysis of the photochemical denitrogenation of **AZ2 g** was difficult due to its low solubility. Clean photochemical denitrogenation of **AZ2 e**, **AZ2 h**, and **16** ($\Phi_{N_2} \approx 0.9$)[23] was observed to quantita-
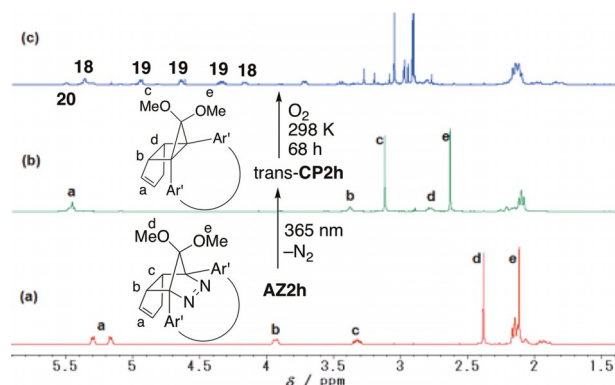
tively produce the corresponding ring-closed compounds *trans*-**CP2 e**, *trans*-**CP2 h**, and *trans*-**17**, respectively (Scheme 2). The *trans*-selective formation of **CP2** as final product was observed at about 298 K, like for S-**DR2 b**.[9n] Compounds *trans*-**CP2 e** and *trans*-**17** with no macrocyclic ring were stable under air and also on silica gel, as confirmed by ^{1}H NMR spectroscopy after isolation of *trans*-**CP2 e** and *trans*-**17** (see the Experimental Section in the Supporting Information). Interestingly, however, *trans*-**CP2 h** with macrocyclic system was highly air sensitive even at 298 K and gave the oxygenated products **18**, **19**, and **20**, which were isolated in yields of 25, 38, and 15, respectively (Figure 6, Scheme 3). The structures of **18**–**20** are quite similar to those of the oxygenated products of compound **21** obtained under air in refluxing benzene,[11a] and their formation suggests that endoperoxide **22** is the intermediate for product formation. The high reactivity of *trans*-**CP2 h** clearly indicates that the C9–C13 σ bond is weakened by the stretching effect induced by the macrocyclic system.
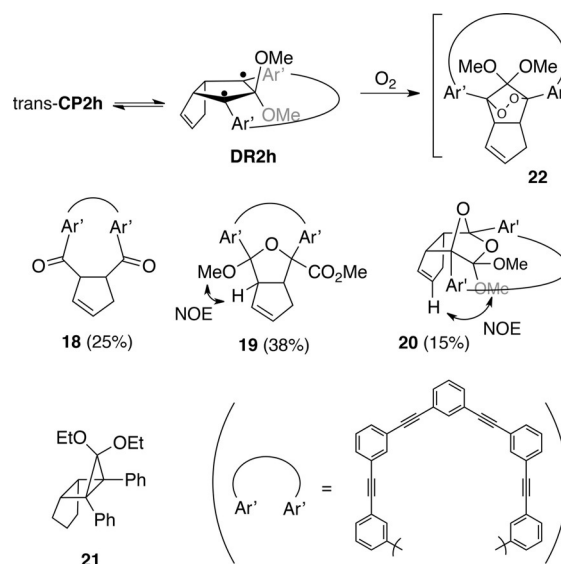
Scheme 3. Intermolecular reaction of **DR2 h** with O_2.

In situ NMR analysis of the photochemical denitrogenation of AZ2 h at 188 K

Gas-phase DFT calculations suggested that S-**DR2 g** has nearly the same in energy as *cis*-**CP2 g** (Table 2). The computational study clarified that *cis* isomers *cis*-**CP2 g,h** are the primary photoproducts of **AZ2 g,h**. Low-temperature in situ NMR analysis at 188 K was conducted for the reaction of **AZ2 h** (3.4 mg, 9.5 mM) in [D_8]toluene under N_2 with 355 nm light from an Nd:YAG laser (Figure 7), which was guided into the NMR cavity by using a quartz rod.[9n, 24] At 188 K, thermally labile species (signals a–d) were observed with *trans*-**CP2 h** (signals e–l) and unconverted **AZ2 h** (signals m–p). After 15 min in the dark, signals a–d disappeared with a concomitant increase of signals e–l (Figure 7), and this suggests that signals a–d are derived from *cis*-**CP2 h** and/or S-**DR2 h**. From the activation parameter found for the decay process of S-**DR2 h** (Table 3), the lifetime of S-

Figure 6. In situ NMR (400 MHz) analysis of the photochemical denitrogenation of **AZ2 h** (10.6 mg, 30 mM) in a sealed NMR tube in [D_6]benzene under degassed conditions with a LED lamp (365 nm) at 298 K. a) ^{1}H NMR spectrum of **AZ2 h** before irradiation. b) ^{1}H NMR spectrum of *trans*-**CP2 h** after 15 min of irradiation. c) ^{1}H NMR spectrum of *trans*-**CP2 h** after 67 h under atmospheric conditions at 298 K.
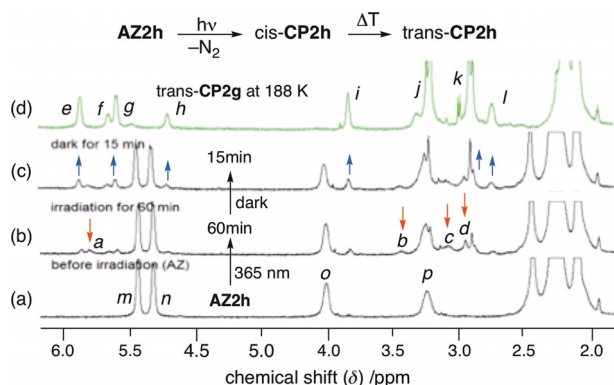
Figure 7. In situ NMR (400 MHz, 2–6 ppm) analysis of the photochemical denitrogenation of a) **AZ2h** (3.4 mg, 9.5 mM) in [D$_8$]toluene under N$_2$ conditions with a Nd:YAG laser (355 nm, 30 mJ) at 188 K after 60 min (b) and after 15 min in the dark (c) and d) *trans*-**CP2h** at 188 K in [D$_8$]toluene.

DR2h should be about 1 s at 188 K; thus, signals a–d do not correspond to S-**DR2h** but to *cis*-**CP2h**. These observations suggest that the DFT calculations overestimate the destabilization energy of **CP2g** and/or the stability of S-**DR2g**. The formation of *cis*-**CP2h** and its thermal isomerization to *trans*-**CP2h** indicate that the primary photoproduct from **AZ2h** included *cis*-**CP2h**. Consistent with the experimental observations, the experimentally determined activation energy of the S-**DR2g** decay process, $E_a = 55.4 \text{ kJ mol}^{-1}$ and $\Delta H^{\ddagger} = 52.9 \text{ kJ mol}^{-1}$ (Table 3), was close to the computed energy barrier of $\Delta E_{ZPE} = 53.1 \text{ kJ mol}^{-1}$ and $\Delta H^{\ddagger} = 50.3 \text{ kJ mol}^{-1}$ involving S-**DR2g** and *cis*-**CP2g** (Table 2).

Conclusions

A new kinetic stabilization (stretch) effect, which is induced by the presence of a macrocyclic ring, was examined in the context of its affecting the reactivity of localized singlet diradicals and their corresponding ring-closed compounds. Extremely long-lived singlet diradicals S-**DR2g,h** ($\tau_{293} \approx 14 \text{ μs}$) emerged in this study. The experimental and computational studies clarified that the distorted triple-bond system in ring-closed compounds **CP2g,h** is central to activating the stretch effect, which kinetically stabilizes the intermediary singlet diradicals **DR2g,h**. The high reactivity of **CP2h** induced by the stretch effect was confirmed by its spontaneous intermolecular reaction with molecular oxygen at 298 K to give oxidation products **18**–**20**. The observed stretch effect may spread to other areas of bond-activation chemistry,[25] such as radical-generation reactions, denitrogenations, and photochromism.

Experimental Section

Full experimental methods including detailed synthetic procedures, characterization data, (NMR, MS, UV/Vis, X-ray crystallography), and DFT calculations (PDF) are available in the Supporting Information.

Acknowledgements

Conflict of interest

The authors declare no conflict of interest.

[1] a) *Reactive Intermediate Chemistry* (Eds.: R. A. Moss, M. S. Platz, M. Jones, Jr.), Wiley, Hoboken, **2004**; b) *Reviews of Reactive Intermediates Chemistry* (Eds.: M. S. Platz, R. A. Moss, M. Jones, Jr.), Wiley, Hoboken, **2007**; c) R. A. Moss, *Chem. Rev.* **2013**, *113*, 6903.

[2] *Excitation Energies and Properties of Open-Shell Singlet Molecules* (Ed.: M. Nakano), Springer, Berlin, **2014**.

[3] *Magnetic Properties of Organic Materials* (Ed.: P. M. Lahti), Marcel Dekker, New York, **1999**.

[4] a) L. J. Johnston, *Chem. Rev.* **1993**, *93*, 251; b) H. Namai, H. Ikeda, Y. Hoshi, N. Kato, Y. Morishita, K. Mizuno, *J. Am. Chem. Soc.* **2007**, *129*, 9032; c) Y. Hattori, T. Kusamoto, H. Nishihara, *Angew. Chem. Int. Ed.* **2014**, *53*, 11845; *Angew. Chem.* **2014**, *126*, 12039.

[5] a) H. Gurer-Orhan, S. Suzen, *Curr. Med. Chem.* **2015**, *22*, 490; b) O. I. Aruoma, *Mutation Research, Fundamental and Molecular Mechanisms of Mutagenesis* **2003**, *523 – 524*, 9.

[6] a) D. Bourissou, O. Guerret, F. P. Gabbaï, G. Bertrand, *Chem. Rev.* **2000**, *100*, 39; b) K. Hirai, H. Tomioka, *Chem. Rev.* **2009**, *109*, 3275; c) J. Vignolle, X. Cattoën, D. Bourissou, *Chem. Rev.* **2009**, *109*, 3333.

[7] R. Hicks, *Stable Radicals: Fundamentals and Applied Aspects of Odd-Electron Compounds*, Wiley, Hoboken, **2010**.

[8] a) W. von E. Doering, V. G. Toscano, G. H. Beasley, *Tetrahedron* **1971**, *27*, 5299; b) J. Kolc, J. Michl, *J. Am. Chem. Soc.* **1973**, *95*, 7391; c) M. J. S. Dewar, L. E. Wade, *J. Am. Chem. Soc.* **1977**, *99*, 4417; d) J. Michl, B. Koutecký, *Tetrahedron* **1988**, *44*, 7559; e) Z. Sun, Z. Zeng, J. Wu, *Acc. Chem. Res.* **2014**, *47*, 2582; f) Z. Zeng, X. Shi, C. Chi, J. T. López Navarrete, J. Casado, J. Wu, *Chem. Soc. Rev.* **2015**, *44*, 6578; g) T. Kubo, *Chem. Lett.* **2015**, *44*, 111; h) S. Li, N. Yuan, Y. Fang, C. Chen, L. Wang, R. Feng, Y. Zhao, H. Cui, X. Wang, *J. Org. Chem.* **2018**, *83*, 3651.

[9] a) T. S. Chambers, G. B. Kistiakowsky, *J. Am. Chem. Soc.* **1933**, *55*, 399; b) R. Hoffmann, *J. Am. Chem. Soc.* **1968**, *90*, 1475; c) L. Salem, C. Rowland, *Angew. Chem. Int. Ed. Engl.* **1972**, *11*, 92; *Angew. Chem.* **1972**, *84*, 86; d) J. A. Berson, L. D. Pedersen, B. K. Carpenter, *J. Am. Chem. Soc.* **1976**, *98*, 122; e) W. T. Borden, in *Diradicals* (Ed.: W. T. Borden) Wiley-Interscience, New York, **1982**, 1; f) V. Bonacic-Koutecky, J. Koutecky, J. Michl, *Angew. Chem. Int. Ed. Engl.* **1987**, *26*, 170; *Angew. Chem.* **1987**, *99*, 216; g) F. Breher, *Coord. Chem. Rev.* **2007**, *251*, 1007; h) M. Abe, J. Ye, M. Mishima, *Chem. Soc. Rev.* **2012**, *41*, 3808; i) M. Abe, *Chem. Rev.* **2013**, *113*, 7011; j) S. J. Getty, D. A. Hrovat, W. T. Borden, *J. Am. Chem. Soc.* **1994**, *116*, 1521; k) W. Adam, W. T. Borden, C. Burda, T. Heidenfelder, M. Jeubes, D. A. Hrovat, F. Kita, S. B. Lewis, D. Scheutzow, J. Wirz, *J. Am. Chem. Soc.* **1998**, *120*, 593; l) M. Abe, W. Adam, W. M. Nau, *J. Am. Chem. Soc.* **1998**, *120*, 11304; m) J. Ye, S. Hatano, M. Abe, R. Kishi, Y. Murata, M. Nakano, W. Adam, *Chem. Eur. J.* **2016**, *22*, 2299; n) M. Abe, S. Tada, T. Mizuno, K. Yamasaki, *J. Phys. Chem. B* **2016**, *120*, 7217; o) M. Abe, K. Kanahara, N. Kadowaki, C.-J. Tan, H.-H.G. Tsai, *Chem. Eur. J.* **2018**, *24*, 7595.

[10] a) D. Scheschkewitz, H. Amii, H. Gornitzka, W. W. Schoeller, D. Bourissou, G. Bertrand, *Science* **2002**, *295*, 1880; b) H. Amii, L. Vranicar, H. Gornitzka, D. Bourissou, G. Bertrand, *J. Am. Chem. Soc.* **2004**, *126*, 1344; c) M. Soleilhavoup, G. Bertrand, *Bull. Chem. Soc. Jpn.* **2007**, *80*, 1241; d) A. Doddi, C. Gemel, M. Winter, R. A. Fischer, C. Goedecke, H. S. Rzepa, G. Frenking, *Angew. Chem. Int. Ed.* **2013**, *52*, 450; *Angew. Chem.* **2013**, *125*, 468; e) E. Niecke, A. Fuchs, F. Baumeister, M. Nieger, W. W. Schoeller,

Angew. Chem. Int. Ed. Engl. **1995**, *34*, 555; *Angew. Chem.* **1995**, *107*, 640; f) H. Sugiyama, S. Ito, M. Yoshifuji, *Angew. Chem. Int. Ed.* **2003**, *42*, 3802; *Angew. Chem.* **2003**, *115*, 3932; g) X. Wang, Y. Peng, M. M. Olmstead, J. C. Fettinger, P. P. Power, *J. Am. Chem. Soc.* **2009**, *131*, 14164; h) K. Takeuchi, M. Ichinohe, A. Sekiguchi, *J. Am. Chem. Soc.* **2011**, *133*, 12478; i) M. Yoshifuji, A. J. Arduengo III, T. A. Konovalova, L. D. Kispert, M. Kikuchi, S. Ito, *Chem. Lett.* **2006**, *35*, 1136; j) C. Cui, M. Brynda, M. M. Olmstead, P. P. Power, *J. Am. Chem. Soc.* **2004**, *126*, 6510; k) H. Cox, P. B. Hitchcock, M. F. Lappert, L. J.-M. Pirssens, *Angew. Chem. Int. Ed.* **2004**, *43*, 4500; *Angew. Chem.* **2004**, *116*, 4600; l) T. Beweries, R. Kuzora, E. Rosenthal, A. Schulz, A. Villinger, *Angew. Chem. Int. Ed.* **2011**, *50*, 8974; *Angew. Chem.* **2011**, *123*, 9136; m) S. Demeshko, C. Godemann, R. Kuzora, A. Schulz, A. Villinger, *Angew. Chem. Int. Ed.* **2013**, *52*, 2105; *Angew. Chem.* **2013**, *125*, 2159.

[11] a) M. Abe, W. Adam, T. Heidenfelder, W. M. Nau, X. Zhang, *J. Am. Chem. Soc.* **2000**, *122*, 2019; b) M. Abe, W. Adam, M. Hara, M. Hattori, T. Majima, M. Nojima, K. Tachibana, S. Tojo, *J. Am. Chem. Soc.* **2002**, *124*, 6540; c) M. Abe, W. Adam, W. T. Borden, M. Hattori, D. A. Hrovat, M. Nojima, K. Nozaki, J. Wirz, *J. Am. Chem. Soc.* **2004**, *126*, 574; d) J. Ye, Y. Fujiwara, M. Abe, *Beilstein J. Org. Chem.* **2013**, *9*, 925.

[12] R. Kishi, Y. Murata, M. Saito, K. Morita, M. Abe, M. Nakano, *J. Phys. Chem. A* **2014**, *118*, 10837.

[13] M. Abe, H. Furunaga, D. Ma, L. Gagliardi, G. Bodwell, *J. Org. Chem.* **2012**, *77*, 7612.

[14] T. Nakagaki, T. Sakai, T. Mizuta, Y. Fujiwara, M. Abe, *Chem. Eur. J.* **2013**, *19*, 10395.

[15] K. Beck, S. Hünig, *Chem. Ber.* **1987**, *120*, 477.

[16] S. Toyota, M. Goichi, M. Kotani, *Angew. Chem. Int. Ed.* **2004**, *43*, 2248; *Angew. Chem.* **2004**, *116*, 2298.

[17] a) P. C. Hariharan, J. A. Pople, *Theor. Chim. Acta* **1973**, *28*, 213; b) A. D. Becke, *J. Chem. Phys.* **1993**, *98*, 5648; c) C. Lee, W. Yang, R. G. Parr, *Phys. Rev. B* **1988**, *37*, 785.

[18] M. Abe, R. Akisaka, *Chem. Lett.* **2017**, *46*, 1586.

[19] W. Adam, H. M. Harrer, F. Kita, W. M. Nau, *Pure Appl. Chem.* **1997**, *69*, 91.

[20] a) J. Zuclich, *J. Chem. Phys.* **1970**, *52*, 3586; b) M. Abe, D. Bégué, H. Santos-Silva, A. Dargelos, C. Wentrup, *Angew. Chem. Int. Ed.* **2018**, *57*, 3212; *Angew. Chem.* **2018**, *130*, 3266 – 3270.

[21] E. T. Harrigan, T. C. Wong, N. Hirota, *J. Chem. Phys.* **1972**, *56*, 1619.

[22] T. Mizuno, M. Abe, N. Ikeda, *Aust. J. Chem.* **2015**, *68*, 1700.

[23] The quantum yield of the photochemical denitrogenation was determined by comparing the rate with that of a standard sample (see ref. [9n]).

[24] S. Geftakis, G. E. Ball, *J. Am. Chem. Soc.* **1998**, *120*, 9953.

[25] In the field of polymer chemistry, a "tension effect" imposed by mechanical forces such as ultrasonic irradiation has been reported to weaken covalent bonds: a) M. K. Beyer, H. Clausen-Schaumann, *Chem. Rev.* **2005**, *105*, 2921; b) C. R. Hickenboth, J. S. Moore, S. R. White, N. R. Sottos, J. Baudry, S. R. Wilson, *Nature* **2007**, *446*, 423; c) I. Park, S. S. Sheiko, S. Nese, K. Matyjaszewski, *Macromolecules* **2009**, *42*, 1805; d) J. M. Lenhardt, A. L. Black, S. L. Craig, *J. Am. Chem. Soc.* **2009**, *131*, 10818; e) D. Wu, J. M. Lenhardt, A. L. Black, B. B. Akhremitchev, S. L. Craig, *J. Am. Chem. Soc.* **2010**, *132*, 15936; f) J. M. Lenhardt, M. T. Ong, R. Choe, C. R. Evenhuis, T. J. Martinez, S. L. Craig, *Science* **2010**, *329*, 1057; g) J. M. Lenhardt, J. W. Ogle, M. T. Ong, R. Choe, T. J. Martinez, S. J. Craig, *J. Am. Chem. Soc.* **2011**, *133*, 3222; h) H. M. Klukovich, Z. S. Kean, S. T. Iacono, S. L. Craig, *J. Am. Chem. Soc.* **2011**, *133*, 17882; i) A. L. Black, J. M. Lenhardt, S. L. Craig, *J. Mater. Chem.* **2011**, *21*, 1655; j) S. Akbulatov, Y. Tian, R. Boulatov, *J. Am. Chem. Soc.* **2012**, *134*, 7620; k) H. M. Klukovich, Z. S. Kean, A. L. Black Ramirez, J. M. Lenhardt, J. Lin, X. Hu, S. L. Sraig, *J. Am. Chem. Soc.* **2012**, *134*, 9577.